

# CHEMISTRY

## A **European** Journal

A Journal of



### Accepted Article

**Title:** Methylsemicarbazide as Ligand in Late 3d Transition Metal Complexes

**Authors:** Joerg Stierstorfer and Norbert Szimhardt

This manuscript has been accepted after peer review and appears as an Accepted Article online prior to editing, proofing, and formal publication of the final Version of Record (VoR). This work is currently citable by using the Digital Object Identifier (DOI) given below. The VoR will be published online in Early View as soon as possible and may be different to this Accepted Article as a result of editing. Readers should obtain the VoR from the journal website shown below when it is published to ensure accuracy of information. The authors are responsible for the content of this Accepted Article.

**To be cited as:** *Chem. Eur. J.* 10.1002/chem.201705030

**Link to VoR:** <http://dx.doi.org/10.1002/chem.201705030>

Supported by  
**ACES**

WILEY-VCH

# Methylsemicarbazide as Ligand in Late 3d Transition Metal Complexes

Norbert Szimhardt and Jörg Stierstorfer\*

**Abstract:** Most ignition and initiation systems nowadays still contain poisonous chemicals such as lead styphnate and lead azide but also chromates and other compounds of high concern. Therefore; methylsemicarbazide (**1**, MSC), which can be prepared in a one-step reaction and an extraordinary high yield of 95 %, has been evaluated as ligand in energetic coordination compounds. For the first time 25 new transition metal complexes ( $Mn^{2+}$ ,  $Ni^{2+}$ ,  $Co^{2+}$ ,  $Cu^{2+}$ , and  $Zn^{2+}$ ) using methylsemicarbazide (**1**) as the ligand were prepared and comprehensively analyzed by e.g. XRD, IR, EA, UV/Vis and DSC/DTA/TGA. Many show a strong energetic character, which can be tuned by using different anions such as  $Cl^-$ ,  $SO_4^{2-}$ ,  $NO_3^-$ ,  $ClO_4^-$ , picrate or styphnate. Selected compounds were additionally evaluated as lead-free primary explosives in initiation tests (nitropenta filled detonators) and in laser ignition systems. Especially compound **7** showed very promising results during these tests and could be a potential candidate for future applications.

## Introduction

The investigation of energetic coordination compounds (ECC) is one of the most useful strategies in discovering new environmentally benign materials for ignition and initiation mixtures.<sup>[1-4]</sup> Ignition implies the release and transfer of energy in the form of heat, flame or subsonic shock waves. This is required for many different applications such as ammunition or in gas generators (e.g. airbags, oxygen candles). Igniters mostly contain a complex mixture of an inorganic pyrotechnic mixture or thermite as well as a weak primary explosive (often lead styphnate (LS) or diazodinitrophenol (DDNP)) and a sensitizer (often tetrazene).<sup>[5]</sup> Owing to their high toxicity and the related pollution of the environment, research into possible replacements is strongly needed.<sup>[6-8]</sup> Various requirements have to be fulfilled when synthesizing suitable candidates. The compound should not only be non-toxic and environmentally friendly but also be easily produced. Depending on the application, the mixtures can be ignited by impact, friction, light, electric impulses or heat. In contrast, initiation mixtures produce hypersonic shock waves, which are able to set of secondary explosives. Until the early 20<sup>th</sup> century, mercury fulminate (MF), first applied by Alfred Nobel, was the initiator of choice (Chart 1).<sup>[9]</sup> Nowadays, usually lead azide

(LA) or silver azide are used. Initiation compositions are used e.g. in millions of commercial detonators for the mining industry but also in nearly all military warheads.

The use of late first row transition metals ( $Mn^{2+}$ ,  $Fe^{2+}$ ,  $Co^{2+}$ ,  $Ni^{2+}$ ,  $Cu^{2+}$ ,  $Zn^{2+}$ ) is a good compromise of (i) availability (ii) price (iii) density (iv) toxicity (only for  $Mn^{2+}$ ,  $Fe^{2+}$ ,  $Cu^{2+}$  and  $Zn^{2+}$ ) and (v) the coordination ability to nitrogen-rich ligands because of low oxophilicity.

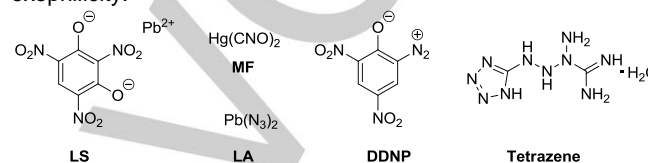


**Chart 1** Molecular structures of lead styphnate (LS), mercury fulminate (MF), lead azide (LA), diazodinitrophenolate (DDNP) and tetrazene.

Useful ECCs contain (a) a metal cation, (b) nitrogen-rich ligands and (c) coordinating or non-coordinating anions (either oxygen-rich such as  $NO_3^-$ ,  $ClO_4^-$ ,  $N(NO_2)_2^-$  or nitrogen-rich such as  $N_3^-$ , tetrazolates or triazolates). Various combinations have been described in the literature.<sup>[10]</sup> Highly energetic and sensitive complexes are formed by the combination of hydrazine derivatives (hydrazine, monomethylhydrazine, dimethylhydrazine, semicarbazide (SC), carbohydrazide (CHZ) but also N-aminoazoles) as the ligand with nitrate or perchlorate transition metal salts.<sup>[11,12]</sup> One of the most prominent ECCs of this type is NHN (nickel hydrazine nitrate) which has also successfully been tested in detonators but contains very toxic nickel(II).<sup>[13]</sup>

Carbohydrazide (CHZ), which belongs to the group of carbazides was first synthesized 1894 by Curtius and Heidenreich who obtained the compound by the reaction of diethyl carbonate with hydrazine.<sup>[14]</sup> Since then, many carbazide-based compounds have been reported (prominent examples in Chart 2a) with manifold uses for example as precursor of drugs<sup>[15]</sup> and herbicides<sup>[16]</sup>. Also various coordination compounds were synthesized using carbazide ligands (Chart 2b) which are proposed to be interesting energetic materials<sup>[17]</sup>. Especially some of them with possible application as primary explosives<sup>[18]</sup> and partly also ignitable by laser irradiation (Chart 2b).<sup>[19]</sup>

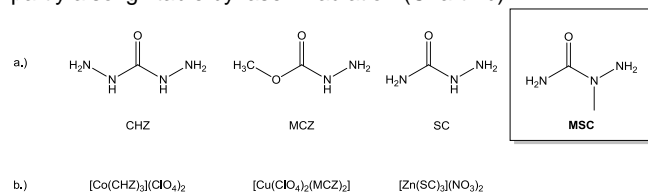


**Chart 2** a.) Overview of selected carbazides; b.) energetic coordination compounds (ECCs) with different carbazide ligands and transition metals.<sup>[20]</sup>

[a] Dr. Jörg Stierstorfer and Norbert Szimhardt, Department of Chemistry, Ludwig Maximilian University of Munich, Butenandtstr. 5-13, D-81377 Munich, Germany, Fax: +49-89-2180-77007, E-mail: jstsch@cup.uni-muenchen.de, Homepage: <http://www.hedm.cup.uni-muenchen.de>

Supporting information (SI) for this article is available on the WWW under <http://www.eurjic.org/> or from the author. SI contains: X-ray Diffraction; IR spectroscopy of **11**, **12**, **15**, **18**, **20** and **23**; DTA plots of **6-8**, **11**, **12**, **15** and **18**; UV-Vis spectra of **6-8**, Experimental part and general methods.

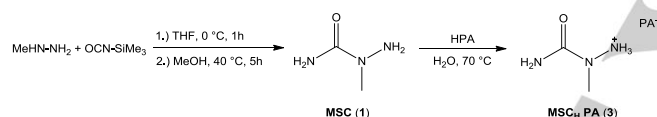
## FULL PAPER

Some of the described CHZ and SC compounds are too sensitive for any potential use. In order to decrease the sensitivity we synthesized methylsemicarbazide (**1**, MSC) as a new ligand for ECCs. MSC has a higher carbon content and has been shown to be an outstanding ligand for the preparation of new energetic material complexes with tunable sensitivities and promising properties.

## Results and Discussion

## Synthesis

The title compound methylsemicarbazide (**1**) can be prepared mainly in two routes starting from different reactants. One way is the reaction of sodium cyanate with methylhydrazine in hydrochloric acid at 0 °C overnight followed by chromatographic purification.<sup>[21]</sup> Another route is the high-yielding reaction of commercially available trimethylsilylisocyanate with methylhydrazine carried out in dry THF (Scheme 1) at a temperature of 0 °C.<sup>[22]</sup> Due to the very hygroscopic character of (trimethylsilyl)isocyanate the reaction mixture was held constant under nitrogen atmosphere. Addition of methanol and heating to 40 °C for 5 hours led to the isolation of **1** with a high yield of 95 %. The acid-base reaction of **1** with picric acid in boiling water resulted in X-ray suitable crystals of the protonated picrate salt **3**.



**Scheme 1** Applied synthesis of methylsemicarbazide (**1**) and its protonated picrate salt (**3**).

Methylsemicarbazide (**1**) bears no acidic proton, which allows the inclusion of the neutral molecule to form complex cations or neutral metal coordination compounds with endothermic (e.g azides) or oxidizing anions like nitrates, perchlorates, picrates (PA) or trinitroresorcinates (HTNR). The selective integration of these anions results in energetic coordination compounds with adjustable sensitivity and performance.

The coordination compounds **4–28** were prepared by the simple reaction of transition metal(II) salts with corresponding equivalents of methylsemicarbazide (**1**) as ligand in water at room or elevated temperatures (Table 1). Due to the good solubility of the resulting complexes only small quantities of solvents were used. In some cases specific amounts of co-solvents like ethanol or acid were added to the reaction mixture in order to get better crystallization behavior, improved yields or higher purities. The concentration of acid used as co-solvent is significant for the formation of the complexes. Excessive amounts of acid, especially for the perchlorate complexes can cause protonation of the methyl-hydrazine moiety and associated

blocking of a coordination site. In this context methylsemicarbazidium perchlorate (**2**) was observed. Another observation was the hydrolysis of methylsemicarbazide (**1**) in too strongly acidic media, which is detected by decomposition products like ammonium perchlorate. Also, in case of the cobalt(II) chloride complexes, two different species have been observed when using varying concentrations of acid. These are the blue water-free compound (**16**) from concentrated hydrochloric acid and a red diaqua complex (**17**) from diluted 2 M acid.

The synthesis of the zinc(II) perchlorate complexes **11** and **12** strongly depends on the stoichiometry of added ligand and yields two different coordination compounds with two or three ligands coordinating to the zinc(II) metal centre, respectively. The corresponding metal(II) salts for the complexes **19–28** were synthesized in situ by reaction of metal(II) carbonates and picric/styphnic acid at 70 °C in water. The colored reaction mixtures were left for crystallization until a solid appeared. All products were filtered off, washed with cold ethanol to remove unreacted starting materials when necessary and dried over night in air. Most of the compounds were obtained in yields of 28–97 % directly from the mother liquor in form of suitable crystals for X-ray determination within hours or days (details are conducted in the experimental part in the SI). Only complexes **20** and **23** precipitated as amorphous powders after the addition of the ligand and all recrystallization attempts failed. A complex formula based on elemental analysis of  $[M^{II}(\text{MSC})_3](\text{PA})_2$  is proposed for compounds **20** and **23**. The majority of the coordination compounds were isolated water-free (without crystal water molecules or aqua ligands) which leads to a higher performance and thermal stability of the compounds. All compounds, except **2** and **16**, could be synthesized and characterized in larger quantities. For the perchlorate salt **2** and the cobalt(II) chlorido complex **16**, unfortunately, only a few single crystals could be picked between unreacted starting material, decomposition products and powder bulk material with unknown constitution. Therefore; only the crystal structures of **2** and **16** could be determined which are shown in the SI. The attempted syntheses of iron(II) and (III) as well as Ag(I) complexes were unsuccessful.

## Crystal structures

The structures of all complexes (except **20** and **23**) were determined by low temperature crystal X-ray diffraction. Details on the crystal structures of compounds **5**, **6**, **9**, **15**, **19**, **21**, **24**, **25**, **27** are given in the SI together with the measurement and refinement data. Single crystals of the zinc(II), manganese(II) and nickel(II) perchlorate complexes **11**, **12**, **15** and **18** were measured to give an indication of the most likely composition. An adequate refinement of the data set was not possible because of the strongly disordered moieties, however elemental analysis confirmed its preliminary observed structures. The coordination

## FULL PAPER

compounds **11/15** and **20/23** exhibit the same coordination environment and their infrared absorptions were therefore compared by infrared spectroscopy (Figure S11/12). The crystal structures were deposited to the CSD database<sup>[23]</sup> and can be obtained free of charge with the CCDC nos. 1534424 (**1**), 1534443 (**2**), 1574510 (**3**), 1534422 (**4**), 1534425 (**5**), 1534426 (**6**), 1534428 (**7**), 1534427 (**8**), 1580445 (**9**), 1534421 (**10**), 1534435 (**13**), 1534440 (**14**), 1534429 (**16**), 1534441 (**17**), 1534429 (**19**),

1574511 (**21**), 1574509 (**22**), 1534442 (**24**), 1534434 (**25**), 1534437 (**26**), 1534420 (**27**), 1534423 (**28**).

Methylsemicarbazide (**1**) crystallizes in the monoclinic space group  $P2_1/n$  with four formula units per unit cell and a calculated density of  $1.288 \text{ g cm}^{-3}$  at 173 K. Selected bond distances and angles of the molecule are given in Figure 1. The C–O ( $1.249(2) \text{ \AA}$ ), C1–N1 ( $1.346(2) \text{ \AA}$ ) and N–N ( $1.414(2) \text{ \AA}$ ) bonds are comparable to values found in carbohydrazide and urea. Lengthening of the C–O double bond comes along with shorter

**Table 1.** Synthesis of transition metal complexes **4–28** with methylsemicarbazide.

Metal Salt	Ligand	co-Anion	Solvent	Conditions	Product	No.
$\text{CuSO}_4 \cdot 5 \text{ H}_2\text{O}$	2 MSC		$\text{H}_2\text{O}$	RT	$[\text{Cu}(\text{H}_2\text{O})_2(\text{MSC})_2]\text{SO}_4$	(4)
$\text{CuCl}_2 \cdot 2 \text{ H}_2\text{O}$	2 MSC		$\text{H}_2\text{O}$ , 15% HCl	RT	$[\text{CuCl}_2(\text{MSC})_2]$	(5)
$\text{Cu}(\text{NO}_3)_2 \cdot 3 \text{ H}_2\text{O}$	2 MSC		$\text{H}_2\text{O}$ , EtOH	RT	$[\text{Cu}(\text{NO}_3)_2(\text{MSC})_2]$	(6)
$\text{Cu}(\text{ClO}_4)_2 \cdot 6 \text{ H}_2\text{O}$	2 MSC		$\text{H}_2\text{O}$ , 70% $\text{HClO}_4$	RT	$[\text{Cu}(\text{ClO}_4)_2(\text{MSC})_2]$	(7)
$\text{CuSO}_4 \cdot 5 \text{ H}_2\text{O}$	1 MSC	2 $\text{NaN}_3$	$\text{H}_2\text{O}$	60 °C, 5 min	$[\text{Cu}(\text{N}_3)_2(\text{MSC})_2]$	(8)
$\text{ZnCl}_2$	2 MSC		$\text{H}_2\text{O}$	RT	$[\text{ZnCl}_2(\text{MSC})_2]$	(9)
$\text{Zn}(\text{NO}_3)_2 \cdot 6 \text{ H}_2\text{O}$	2 MSC		$\text{H}_2\text{O}$ , EtOH	RT	$[\text{Zn}(\text{NO}_3)_2(\text{MSC})_2]$	(10)
$\text{Zn}(\text{ClO}_4)_2 \cdot 6 \text{ H}_2\text{O}$	2 MSC		$\text{H}_2\text{O}$	RT	$[\text{Zn}(\text{H}_2\text{O})_2(\text{MSC})_2](\text{ClO}_4)_2$	(11)
$\text{Zn}(\text{ClO}_4)_2 \cdot 6 \text{ H}_2\text{O}$	3 MSC		$\text{H}_2\text{O}$	RT	$[\text{Zn}(\text{MSC})_3](\text{ClO}_4)_2 \cdot \text{H}_2\text{O}$	(12)
$\text{MnCl}_2 \cdot 2 \text{ H}_2\text{O}$	2 MSC		$\text{H}_2\text{O}$	RT	$[\text{MnCl}_2(\text{MSC})_2]$	(13)
$\text{Mn}(\text{NO}_3)_2 \cdot 4 \text{ H}_2\text{O}$	2 MSC		$\text{H}_2\text{O}$	RT	$[\text{Mn}(\text{NO}_3)_2(\text{MSC})_2]$	(14)
$\text{Mn}(\text{ClO}_4)_2 \cdot 6 \text{ H}_2\text{O}$	2 MSC		$\text{H}_2\text{O}$	RT	$[\text{Mn}(\text{H}_2\text{O})_2(\text{MSC})_2](\text{ClO}_4)_2$	(15)
$\text{CoCl}_2 \cdot 6 \text{ H}_2\text{O}$	2 MSC		$\text{H}_2\text{O}$ , conc. HCl	RT	$[\text{CoCl}_2(\text{MSC})_2]$	(16)
$\text{CoCl}_2 \cdot 6 \text{ H}_2\text{O}$	2 MSC		$\text{H}_2\text{O}$ , 2M HCl	RT	$[\text{Co}(\text{H}_2\text{O})_2(\text{MSC})_2]\text{Cl}_2$	(17)
$\text{Ni}(\text{ClO}_4)_2 \cdot 6 \text{ H}_2\text{O}$	3 MSC		$\text{H}_2\text{O}$	50 °C, 5 min	$[\text{Ni}(\text{MSC})_3](\text{ClO}_4)_2$	(18)
$\text{CuCO}_3$	2 MSC	2 HPA	$\text{H}_2\text{O}$	70 °C, 5 min	$[\text{Cu}(\text{PA})_2(\text{MSC})_2]$	(19)
$\text{ZnCO}_3 \cdot 3 \text{ Zn}(\text{OH})_2$	12 MSC	2 HPA	$\text{H}_2\text{O}$	70 °C, 5 min	$[\text{Zn}(\text{MSC})_3](\text{PA})_2$	(20)
$\text{MnCO}_3$	2 MSC	2 HPA	$\text{H}_2\text{O}$	70 °C, 5 min	$[\text{Mn}(\text{PA})_2(\text{MSC})_2]$	(21)
$\text{CoCO}_3 \cdot \text{H}_2\text{O}$	2 MSC	2 $\text{H}_2\text{TNR}$	$\text{H}_2\text{O}$	70 °C, 5 min	$[\text{Co}(\text{PA})_2(\text{MSC})_2]$	(22)
$\text{NiCO}_3 \cdot 2 \text{ Ni}(\text{OH})_2 \cdot 4 \text{ H}_2\text{O}$	9 MSC	2 $\text{H}_2\text{TNR}$	$\text{H}_2\text{O}$	70 °C, 5 min	$[\text{Ni}(\text{MSC})_3](\text{PA})_2$	(23)
$\text{CuCO}_3$	2 MSC	2 $\text{H}_2\text{TNR}$	$\text{H}_2\text{O}$	70 °C, 5 min	$[\text{Cu}(\text{H}_2\text{O})_2(\text{MSC})_2](\text{HTNR})_2$	(24)
$\text{ZnCO}_3 \cdot 3 \text{ Zn}(\text{OH})_2$	8 MSC	2 $\text{H}_2\text{TNR}$	$\text{H}_2\text{O}$	70 °C, 5 min	$[\text{Zn}(\text{H}_2\text{O})_2(\text{MSC})_2](\text{HTNR})_2$	(25)
$\text{MnCO}_3$	2 MSC	2 $\text{H}_2\text{TNR}$	$\text{H}_2\text{O}$	70 °C, 5 min	$[\text{Mn}(\text{HTNR})_2(\text{MSC})_2]$	(26)
$\text{CoCO}_3 \cdot \text{H}_2\text{O}$	2 MSC	2 $\text{H}_2\text{TNR}$	$\text{H}_2\text{O}$	70 °C, 5 min	$[\text{Co}(\text{H}_2\text{O})_2(\text{MSC})_2](\text{HTNR})_2$	(27)
$\text{NiCO}_3 \cdot 2 \text{ Ni}(\text{OH})_2 \cdot 4 \text{ H}_2\text{O}$	6 MSC	2 $\text{H}_2\text{TNR}$	$\text{H}_2\text{O}$	70 °C, 5 min	$[\text{Ni}(\text{H}_2\text{O})_2(\text{MSC})_2](\text{HTNR})_2$	(28)

C–N and N–N single bond distances and confirms the conjugation of these atoms.<sup>[24,25]</sup> In addition, stabilization of the molecular structure is generated through strong intermolecular hydrogen

bonds formed between the carbonyl function and the neighboring amino groups (N1–H1B••O1  $0.93(2)$ ,  $2.02(2)$ ,  $2.9428(19) \text{ \AA}$ ,  $172(17)^\circ$ ; N3–H3A••O1  $0.947(18)$ ,  $2.052(18)$ ,  $2.9920(19) \text{ \AA}$ ,

## FULL PAPER

171.7(15)°, N3–H3B••O1 0.91(2), 2.25(2), 3.148(2) Å, 172.5(16)°. These observations are consistent with the almost planar geometry of the molecule ( $\angle$  (N3–N2–C1–N1) =  $-5.8(2)^\circ$ ;  $\angle$  (C2–N2–C1–O1) =  $6.9(2)^\circ$ ).

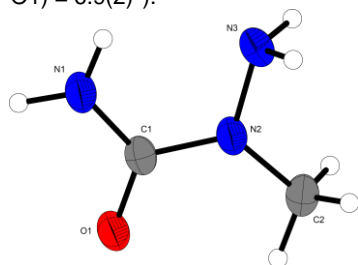


**Figure 1** Molecular structure of methylsemicarbazide (**1**). Thermal ellipsoids of non-hydrogen atoms in all structures are set to the 50% probability level. Selected bond lengths (Å): O1–C1 1.249(2), N1–C1 1.346(2), N2–N3 1.414(2), N2–C1 1.349(2), N2–C2 1.445(2); selected bond angles ( $^\circ$ ): N3–N2–C1 117.81(2), N1–C1–N2 117.26(2), N3–N2–C2 119.20(2), O1–C1–N1 121.40(2), C1–N2–C2 122.26(2), O1–C1–N2 121.28(2); selected torsion angles ( $^\circ$ ): N3–N2–C1–N1  $-5.8(2)$ , C2–N2–C1–O1  $6.9(2)$ .

As described above, parent compound **1** can be protonated under certain acidic conditions. Protonation takes place on the  $\text{NH}_2$  group of the methylhydrazine functional group and causes a reorientation of half of the molecule. The salts show significantly higher densities in comparison to the neutral molecule (**2**:  $1.734 \text{ g cm}^{-3}$  (123 K); **3**:  $1.750 \text{ g cm}^{-3}$  (143 K) vs.  $1.288 \text{ g cm}^{-3}$  (173 K) for **1**). The perchlorate compound **2** crystallizes in the monoclinic space group  $P2_1/c$  with sixteen formula units per unit cell. On the other hand the picrate salt **3** crystallizes in the triclinic space group  $P\bar{1}$  with two molecules in the unit cell. Structural parameters and the molecular structures of both salts are shown in Figure 2. Salt formation had no significant influence on the bond distances but rather on the planarity of the methylsemicarbazinium cation with a torsion angle of  $\angle$  (C2–N2–C1–N3) =  $-30.1(6)^\circ$  in **3**.

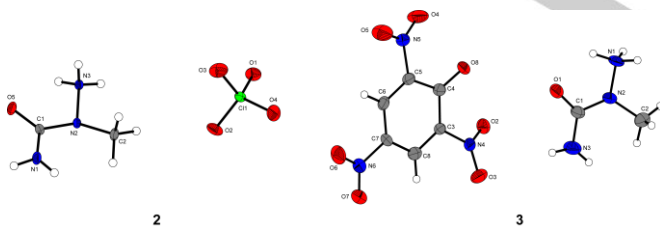


**Figure 2** Molecular moieties of the MSC salts **2** (left) and **3** (right). Selected bond lengths (Å): **2**: N1–C1 1.325(4), N2–N3 1.430(3), N2–C2 1.464(4), N2–C1 1.386(4), C1–O5 1.238(4), C1–O1 1.438(2); **3**: N1–N2 1.446(5), N2–C1 1.405(5), N2–C2 1.457(6), N3–C1 1.322(6), C1–O1 1.228(6); selected bond angles ( $^\circ$ ): **2**: N3–N2–C1 111.3(2), N3–N2–C2 112.9(2), C1–N2–C2 124.2(2), O1–C1–N1 125.1(3), O1–C1–N2 118.0(3); **3**: N1–N2–C1 110.5(3), N1–N2–C2 112.9(3), C1–N2–C2 122.9(2), O1–C1–N2 119.7(4), O1–C1–N3 124.3(4); selected torsion angle ( $^\circ$ ): **3**: C2–N2–C1–N3  $-30.1(6)$ .

The bond distances and most angles of the coordinating MSC ligands in the examined coordination compounds are similar to the non-coordinated ligand **1**. The carbazide ligand is therefore not investigated or discussed in more detail in any of the compounds crystal structures outlined below. Methylsemicarbazide (**1**) is bidentate and coordinates through the carbonyl oxygen and amino-methylhydrazine nitrogen atom to the

transition metal. A reorientation of the MSC molecule, already described in the salts **2** and **3**, can be observed in the complexes (Chart 3). All complexes show a (more or less) octahedral coordination sphere, which can be explained by the low steric hindrance of the ligand.

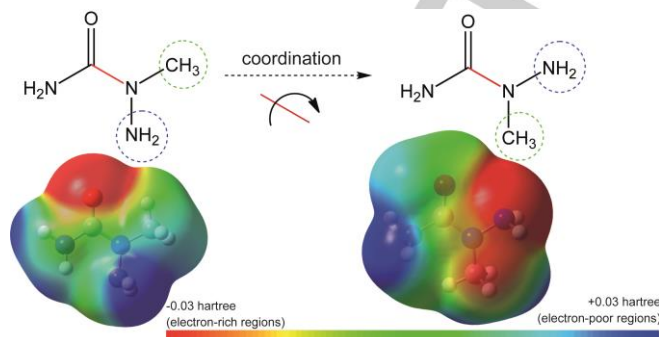


**Chart 3** Reorientation of the MSC molecule after coordination or salt formation and depiction of the calculated (B3LYP / 6-31G(d,p)) electrostatic potentials (3D isosurface of electron density) of **1** and its coordinated form.

The copper(II) sulfate complex **4** crystallizes in the form of blue rods in the monoclinic space group  $P2_1/c$  with four formula units per unit cell and a calculated density of  $1.857 \text{ g cm}^{-3}$  at 123 K. The molecular unit shown in Figure 3 consists of an octahedrally surrounded copper(II) center with two aqua ligands along the Jahn-Teller distorted axial axis (Cu1–O8 =  $2.495(3) \text{ \AA}$ ) and two bidentately connected MSC ligands in a plane (Cu1–O5 =  $1.934(3) \text{ \AA}$ , Cu1–N2 =  $1.977(4) \text{ \AA}$ ,  $\angle$  (O5–Cu1–N2) =  $83.28(1)^\circ$ ,  $\angle$  (O5–Cu1–N2 $^i$ ) =  $96.73(12)^\circ$ ). All complexes described here show higher densities than the non-coordinating MSC molecule itself.

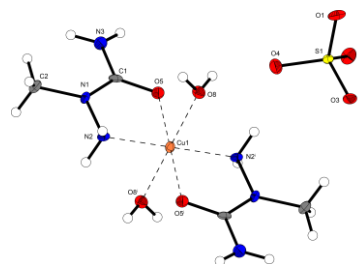


**Figure 3** Molecular unit of  $[\text{Cu}(\text{H}_2\text{O})_2(\text{MSC})_2]\text{SO}_4$  (**4**). Selected bond lengths (Å): Cu1–O5 1.934(3), Cu1–O8 2.495(3), Cu1–N2 1.977(4), S1–O1 1.467(3); selected bond angles ( $^\circ$ ): O5–Cu1–O8 88.03(11), O5–Cu1–N2 83.28(12), O8–Cu1–N2 90.26(12), O5–Cu1–O8 $^i$  91.97(11), O5–Cu1–N2 $^i$  96.73(12), O1–S1–O2 109.77(16). Symmetry code: (i)  $-x, -y, -z$ .

Complexes **5** (copper(II), green block, Figure S1), **9** (zinc(II), colorless block, Figure S2) and **16** (cobalt(II), blue block) with coordinating chlorido ligands crystallize in the monoclinic space group  $P2_1/c$  with two formula units per unit cell showing similar densities (**5**:  $1.838 \text{ g cm}^{-3}$  at 123 K; **9**:  $1.799 \text{ g cm}^{-3}$  and **16**:  $1.791 \text{ g cm}^{-3}$  at 123 K). The remaining complex **13** with coordinating chlorido ligands and manganese(II) transition metal center (colorless block, Figure S3) also crystallizes in a monoclinic space group ( $P2_1/n$ ) with four formula units per unit cell and exhibits a calculated density of  $1.765 \text{ g cm}^{-3}$  at 173 K.

## FULL PAPER

Every metal(II) center, as illustrated for compound **16** (Figure 4), shows an octahedral surrounding with two chloridos and two methylsemicarbazides. On the contrary, the cobalt(II) chloride complex **17** is composed of two aqua ligands and two MSC ligands. The chlorides act only as counter-anions (Figure 4). It crystallizes in the monoclinic space group  $P2_1/n$  with four formula units per unit cell and has a calculated density of  $1.735 \text{ g cm}^{-3}$  at 123 K.

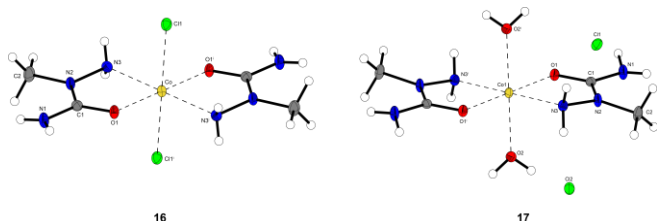


**Figure 4** Complex units of compound **16** (left) and **17** (right). Selected coordination distances (Å): **16**: Co–Cl1 2.4935(6), Co1–O1 2.0396(16), Co1–N3 2.140(2); **17**: Co1–O2 2.1016(17), Co1–N3 2.138(2), Co1–O3 2.0505(16); selected bond angles (°): **16**: Cl1–Co–O1 88.48(5), Cl1–Co–N3 91.22(7), Cl1–Co–O1<sup>i</sup> 91.53(5), Cl1–Co–N3<sup>i</sup> 88.78(7), O1–Co–N3 78.46(8), O1–Co–N3<sup>i</sup> 101.54(8); **17**: O2–Co1–O1 91.09(2), O2–Co1–N3 88.67(2), O1–Co1–N3 78.06(2), N3–Co1–O1 101.94(2). Symmetry codes: **16**: (i) 1–x, –y, 1–z; **17**: (i) 1–x, 1–y, 1–z.

The copper(II) and manganese(II) nitrate complexes **6/14** crystallize isotypically in the triclinic space group  $P\bar{1}$  with one formula unit per unit cell (**6**: blue block,  $1.873 \text{ g cm}^{-3}$ ; **14**: colorless block,  $1.752 \text{ g cm}^{-3}$  at 173 K). The colorless zinc(II) nitrate compound **10** crystallizes in the monoclinic space group  $P2_1$  with two formula units per unit cell and a calculated density of  $1.860 \text{ g cm}^{-3}$  (123 K). Each metal(II) cation is bonded to two nitrate ligands in axial positions and two MSC ligands in equatorial positions. As expected, the  $d^9$ -copper(II) center shows Jahn-Teller distortion (elongation in axial direction). Their molecular motifs are illustrated in Figure 5 and S4.

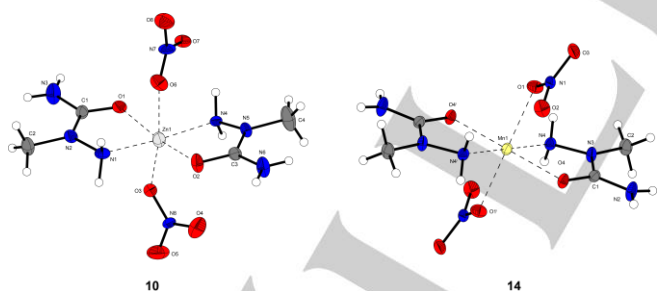


**Figure 5** Molecular units of compounds **10** (left) and **14** (right). Selected coordination distances (Å): **10**: Zn1–O1 2.061(6), Zn1–O2 2.046(6), Zn1–O3 2.145(9), Zn1–O6 2.351(9), Zn1–N1 2.073(10), Zn1–N4 2.092(9); **14**: Mn1–O1 2.2176(17), Mn1–N4 2.268(2), Mn1–O4 2.1392(15); selected bond angles (°): **10**: O1–Zn1–O2 169.2(4), O1–Zn1–O3 88.7(3), O1–Zn1–O6 85.8(3), O1–Zn1–N1 78.9(4), O1–Zn1–N4 100.5(3), O2–Zn1–O3 102.0(4), O2–Zn1–O6 83.5(4), O2–Zn1–N1 99.5(4), O2–Zn1–N4 80.3(4), O3–Zn1–O6 172.5(3), O3–Zn1–N1 87.9(4), O3–Zn1–N4 97.1(3), O6–Zn1–N1 86.1(4), O6–Zn1–N4 89.0(3), N1–Zn1–N4 175.0(4); **14**: O1–Mn1–O4 89.53(5), O1–Mn1–N4 83.80(7), O1–Mn1–O4<sup>i</sup> 90.47(5), O1–Mn1–N4<sup>i</sup> 96.20(7), O4–Mn1–N4 73.24(6), O4–Mn1–N4<sup>i</sup> 106.76(6). Symmetry code: **14**: (i) 2–x, –y, 2–z.

From an energetic perspective very interesting, the copper(II) perchlorate complex **7** is octahedrally coordinated by two perchlorate ligands in Jahn-Teller distorted axial positions and by two chelating MSC ligands in a plane (Figure 6). It crystallizes in the form of blue blocks in the monoclinic space group  $P2_1/c$  with two formula units per unit cell and the highest calculated density of  $2.055 \text{ g cm}^{-3}$  at 123 K of all complexes described here.

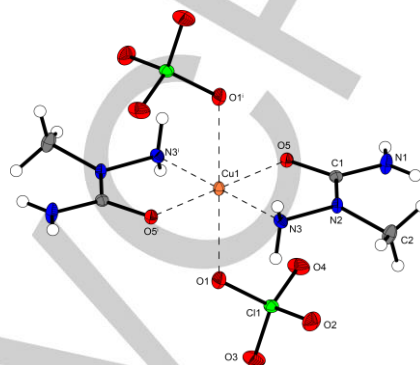


**Figure 6** Complex unit of the highly energetic complex  $[\text{Cu}(\text{ClO}_4)_2(\text{MSC})_2]$  (**7**). Selected bond lengths (Å): Cu1–O1 2.4730(16), Cu1–O5 1.9257(15), Cu1–N3 1.994(2), Cl1–O1 1.4472(16); selected bond angles (°): O1–Cu1–O5 91.41(6), O1–Cu1–N3 90.07(7), O1–Cu1–O5<sup>i</sup> 88.59(6), O1–Cu1–N3<sup>i</sup> 89.93(7), O5–Cu1–N3 82.83(8), O5–Cu1–N3<sup>i</sup> 97.17(8), O1–Cl1–O2 108.57(11). Symmetry code: (i) 2–x, –y, 1–z.

Copper(II) azido complex **8** crystallizes in the form of green needles in the monoclinic space group  $P2_1/c$  with four formula units per unit cell and a calculated density of  $2.016 \text{ g cm}^{-3}$  at 123 K. Every copper(II) center is hexa-coordinated by one chelating MSC molecule and four bridging azido ligands forming polymeric chains. It is the only octahedral complex with just one methylsemicarbazide ligand coordinating to the metal(II) center. Due to the  $d^9$ -induced Jahn-Teller distortion, elongation along the axial sites can be observed, which are occupied by azido ligands ( $\text{Cu1–N6}^{\text{ii}} = 2.636(3) \text{ Å}$ ,  $\text{Cu1–N9}^{\text{i}} = 2.479(2) \text{ Å}$ ). The coordination environment of the copper(II) cation is depicted in Figure 7a and shows the small deviation of the ideal coordination sphere caused by the fixed structure of the azidos and the MSC ligand ( $\angle(\text{O1–Cu1–N3}) = 81.52(7)^\circ$ ,  $\angle(\text{N3–Cu1–N6}^{\text{ii}}) = 78.03(10)^\circ$ ). Various coordination and bridging modes of the azido ligands (1,1; 1,3; 1,1,3; 1,1,1 etc.) are possible and known in literature.<sup>[26]</sup> The azido ligand N4–N5–N6 connects two copper(II) centers through cis 1,3-coordination while trans 1,3-coordination can be observed for the second azido equivalent N7–N8–N9 (Figure 7b). This end-on binding situation causes similar bond lengths and almost linear bond angles within the azido groups ( $\text{N4–N5} = 1.204(3) \text{ Å}$ ,  $\text{N5–N6} = 1.162(3) \text{ Å}$ ,  $\text{N7–N8} = 1.195(3) \text{ Å}$ ,  $\text{N8–N9} = 1.160(4) \text{ Å}$ ,  $\angle(\text{N4–N5–N6}) = 176.4(3)^\circ$ ,  $\angle(\text{N7–N8–N9}) = 179.6(3)^\circ$ ).

## FULL PAPER

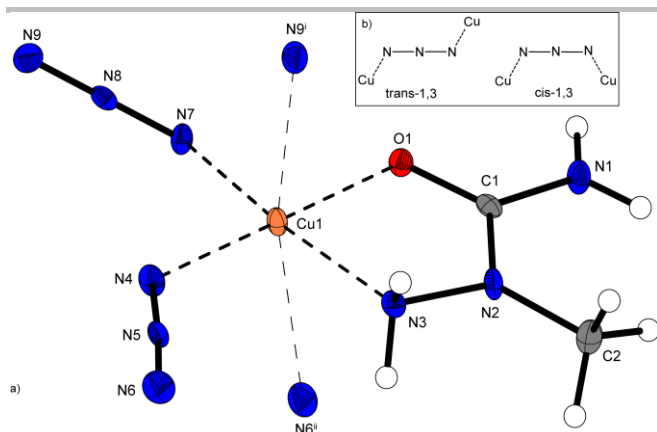


**Figure 7** a.) Depiction of the octahedral coordination environment of the copper(II) cation in **8**. Selected bond lengths (Å): Cu1–O1 1.957(2), Cu1–N3 2.012(3), Cu1–N4 1.963(3), Cu1–N7 1.988(2), Cu1–N6<sup>ii</sup> 2.636(3), Cu1–N9<sup>i</sup> 2.479(2), N4–N5 1.204(3), N5–N6 1.162(3), N7–N8 1.195(3), N8–N9 1.160(4); selected bond angles (°): O1–Cu1–N3 81.52(9), O1–Cu1–N4 179.24(9), O1–Cu1–N7 88.72(9), O1–Cu1–N6<sup>ii</sup> 85.14(9), O1–Cu1–N9<sup>i</sup> 86.59(9), N3–Cu1–N4 99.15(10), N3–Cu1–N7 169.26(10), N3–Cu1–N6<sup>ii</sup> 78.03(10), N3–Cu1–N9<sup>i</sup> 92.01(10), N4–Cu1–N7 90.58(10), N4–Cu1–N6<sup>ii</sup> 94.63(11), N4–Cu1–N9<sup>i</sup> 93.75(11), N6<sup>ii</sup>–Cu1–N7 96.77(9), N7–Cu1–N9<sup>i</sup> 91.88(9), N6<sup>ii</sup>–Cu1–N9<sup>i</sup> 167.88(8), N4–N5–N6 176.4(3), N7–N8–N9 179.6(3). Symmetry codes: (i) 2.5–x, –0.5+y, 0.5–z; (ii) 1.5–x, 0.5+y, 0.5–z; b.) Observed coordination modes of the azido ligand in **8**.

The water-free copper(II) **19** (green block), manganese(II) **21** (yellow block) and cobalt(II) **22** (orange block) picrate complexes crystallize isotypically to each other in the triclinic space group *P*–1 with one formula unit per unit cell exhibiting very similar calculated densities (**19**: 1.885 g cm<sup>–3</sup> at 123 K; **21**: 1.825 g cm<sup>–3</sup> and **22**: 1.866 g cm<sup>–3</sup> at 143 K) and cell dimensions. Their molecular unit consist of two chelating MSC ligands and two picrate ligands in axial positions (Figure S5/6 and 8). The picrate anion binds via its deprotonated phenolate-group to the transition metal(II) in a monodentate way causing shortening of the MSC bond angle due to the steric hindrance of the trinitrobenzene derivative (< O1–Co1–N3) = 77.42(7)°).

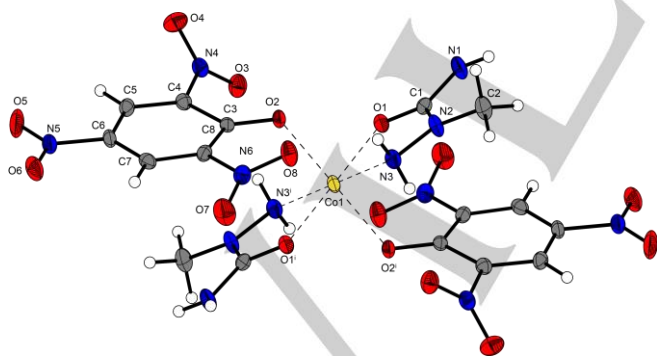


**Figure 8** Molecular unit of the cobalt(II) picrate complex **22**. Selected bond lengths (Å): Co1–O1 2.0664(15), Co1–O2 2.1136(13), Co1–N3 2.115(2); selected bond angles (°): O1–Co1–O2 90.36(6), O1–Co1–N3 77.42(7), O1–Co1–O2<sup>i</sup> 89.64(5), O1–Co1–N3<sup>i</sup> 102.58(7), O2–Co1–N3 89.26(7), O2–Co1–N3<sup>i</sup> 90.74(7). Symmetry code: (i) 1–x, 1–y, –z.

In comparison to the picrate compounds discussed so far, the styphnate counter-anions do not coordinate to the transition

metals(II) in compounds **24/25** and **27/28**, which crystallize isotypically in the triclinic space group *P*–1 with one formula unit per unit cell and analogous cell parameters. Their densities increase in the row of Ni<sup>2+</sup> (1.844 g cm<sup>–3</sup>; 173 K) < Co<sup>2+</sup> (1.852 g cm<sup>–3</sup>; 123 K) < Zn<sup>2+</sup> (1.866 g cm<sup>–3</sup>; 123 K) < Cu<sup>2+</sup> (1.880 g cm<sup>–3</sup>; 173 K). The molecular unit of the complexes illustrated in Figure 9 and in the SI are built up by two aqua ligands, two MSC ligands and two non-coordinating styphnates. The space group *P*–1 could also be determined for the water-free manganese(II) picrate complex **26** (1.892 g cm<sup>–3</sup> at 123 K), which shows a different molecular composition with no aqua ligands, but two coordinating styphnate ligands instead (Figure 9). A similar situation that was found for the picrates with distortion along the MSC bond angle can also be observed for the styphnate coordination compounds. Each copper(II) complex in **19** and **24** show Jahn-Teller distortion with longer axial bond distances.

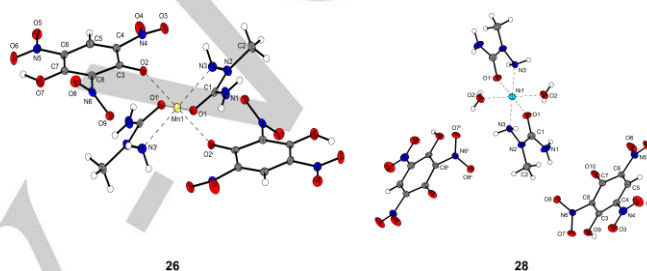


**Figure 9** Complex units of compounds **26** (left) and **28** (right). Selected coordination distances (Å): **26**: Mn1–O1 2.1426(15), Mn1–O2 2.1949(15), Mn1–N3 2.266(2); **28**: Ni1–N3 2.060(3), Ni1–O1 1.9923(15), Ni1–O2 2.143(2); selected bond angles (°): **26**: O1–Mn1–O2 90.51(6), O1–Mn1–N3 73.19(7), O1–Mn1–O2<sup>i</sup> 89.46(6), O1–Mn1–N3<sup>i</sup> 106.81(7), O2–Mn1–N3 91.45(7), O1<sup>i</sup>–Mn1–O2 89.49(6), O2–Mn1–N3<sup>i</sup> 88.55(7); **28**: O1–Ni1–O2<sup>i</sup> 91.30(8), O1–Ni1–N3<sup>i</sup> 99.43(8), O2–Ni1–N3 85.23(9), O2–Ni1–N3<sup>i</sup> 94.78(9), O1<sup>i</sup>–Ni1–O2<sup>i</sup> 88.70(8), O1<sup>i</sup>–Ni1–N3<sup>i</sup> 80.57(8). Symmetry codes: **26**: (i) 1–x, 1–y, –z; **28**: (i) –x, –y, 1–z; (ii) 1–x, 1–y, 1–z.

### Sensitivities and Thermal Stability

Thermal stability measurements of highly sensitive and sensitive coordination compounds are very challenging since quantities larger than ~2 mg can damage the instrument seriously. On the other hand, endothermic signals such as melting, vaporization, dehydration or loss of ligand may not be detected properly when using an inadequate amount. Approximately 1 mg of the compounds were measured with a heating rate of 5 °C min<sup>–1</sup> via differential thermal analysis (DTA) and/or by thermal gravimetric analysis (TGA). Critical temperatures are give as onset temperatures and are summarized in Table 2. Additional details on the DTA plots of **6–8**, **11**, **12**, **15** and **18** are given in the Supporting Information. The majority of the investigated compounds have exothermic decomposition events higher or close to 180 °C. Losses of water or ligands expressed by endothermic decomposition points have been observed partly at lower temperatures. Methylsemicarbazide (**1**) showed no exothermic decomposition event in the measured range of 25–400 °C but had indeed two endothermic points. Compound **1** first melts (60 °C) and vaporizes afterwards at temperatures above 110 °C, which was determined by constant weight loss during TGA (Figure 10). This behaviour

## FULL PAPER

could be a possible explanation for the exceptional endothermic peaks observed for **5**, **9**, **10**, **12–14**, **17** and **18** during DTA measurements. Endothermic loss of coordinating MSC molecules could lead to the formation of intermediate species, which decompose in an exothermic manner at later stages. Numerous decomposition paths and mechanisms are possible. Similar phenomena have already been described in the literature.<sup>[27–29]</sup> The ligand vaporization tendency and the relating bond strengths are strongly influenced by the metal ( $\text{Zn}(\text{ClO}_4)_2$  (**12**) vs.  $\text{Ni}(\text{ClO}_4)_2$  (**18**), Figure S12), anion ( $\text{Cu}(\text{NO}_3)_2$  (**6**) vs.  $\text{Cu}(\text{ClO}_4)_2$  (**19**), Figure S12) and the corresponding coordination environment ( $\text{Zn}(\text{ClO}_4)_2$ , (**11**) vs. (**12**)). The copper(II) azido (Figure 10) and nitrate complexes **6** and **8**, which decompose exothermically at low temperatures of 121 °C (**8**) and 147 °C (**6**) showed the lowest thermal stabilities of all investigated coordination compounds. Comparing them to the other complexes bearing different anions, but the same metal ion, the decomposition temperatures increase in the following order:  $\text{N}_3^-$  (121 °C) <  $\text{NO}_3^-$  (146 °C) <  $\text{SO}_4^{2-}$  (156 °C) <  $\text{Cl}^-$  (166 °C) <  $\text{PA}^-$  (179 °C)  $\approx$   $\text{HTNR}^-$  (179 °C) <  $\text{ClO}_4^-$  (186 °C). This general trend underlines the importance and correlation of the decomposition temperature with the anion and coordination environment.

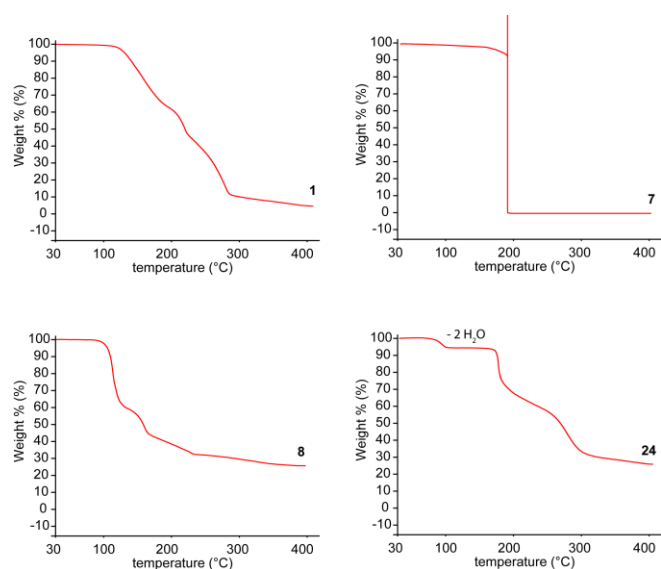


**Figure 10** TGA measurements of the free ligand **1** and selected complexes at a heating rate of 5 °C min<sup>-1</sup>.

The water-free metal(II) MSC picrate coordination compounds showed relatively high thermal stabilities ranging from 179 °C for **19** up to 217 °C for **23** (Figure 11). Their exothermic decomposition temperatures increase in the following order:  $\text{Cu}^{2+}$  (179 °C) <  $\text{Zn}^{2+}$  (190 °C)  $\approx$   $\text{Mn}^{2+}$  (190 °C) <  $\text{Co}^{2+}$  (211 °C) <  $\text{Ni}^{2+}$  (217 °C). For previous complexes analogous trends have been observed.<sup>[30]</sup>

**Table 2.** Thermal stability measurements of **1**, **3–15** and **17–28** by DTA.

	$T_{\text{endot.}}$ (°C) <sup>[a]</sup>	$T_{\text{endo2.}}$ (°C) <sup>[a]</sup>	$T_{\text{exo.}}$ (°C) <sup>[b]</sup>
<b>MSC (1)</b>	60	111	—
<b>MSC<sub>H</sub> PA (3)</b>	—	—	166
<b>[Cu(H<sub>2</sub>O)<sub>2</sub>(MSC)<sub>2</sub>]SO<sub>4</sub> (4)</b>	144	—	156
<b>[CuCl<sub>2</sub>(MSC)<sub>2</sub>] (5)</b>	146	—	166
<b>[Cu(NO<sub>3</sub>)<sub>2</sub>(MSC)<sub>2</sub>] (6)</b>	—	—	147
<b>[Cu(ClO<sub>4</sub>)<sub>2</sub>(MSC)<sub>2</sub>] (7)</b>	—	—	186
<b>[Cu(N<sub>3</sub>)<sub>2</sub>(MSC)] (8)</b>	—	—	121
<b>[ZnCl<sub>2</sub>(MSC)<sub>2</sub>] (9)</b>	171	—	186
<b>[Zn(NO<sub>3</sub>)<sub>2</sub>(MSC)<sub>2</sub>] (10)</b>	183	—	208
<b>[Zn(H<sub>2</sub>O)<sub>2</sub>(MSC)<sub>2</sub>](ClO<sub>4</sub>)<sub>2</sub> (11)</b>	114	—	231
<b>[Zn(MSC)<sub>3</sub>](ClO<sub>4</sub>)<sub>2</sub> · H<sub>2</sub>O (12)</b>	123	187	333
<b>[MnCl<sub>2</sub>(MSC)<sub>2</sub>] (13)</b>	107	189	209
<b>[Mn(NO<sub>3</sub>)<sub>2</sub>(MSC)<sub>2</sub>] (14)</b>	169	—	208
<b>[Mn(H<sub>2</sub>O)<sub>2</sub>(MSC)<sub>2</sub>](ClO<sub>4</sub>)<sub>2</sub> (15)</b>	96	—	234
<b>[Co(H<sub>2</sub>O)<sub>2</sub>(MSC)<sub>2</sub>]Cl<sub>2</sub> (17)</b>	99	259	266
<b>[Ni(MSC)<sub>3</sub>](ClO<sub>4</sub>)<sub>2</sub> (18)</b>	252	—	258
<b>[Cu(PA)<sub>2</sub>(MSC)<sub>2</sub>] (19)</b>	—	—	179
<b>[Zn(MSC)<sub>3</sub>](PA)<sub>2</sub> (20)</b>	—	—	190
<b>[Mn(PA)<sub>2</sub>(MSC)<sub>2</sub>] (21)</b>	—	—	190
<b>[Co(PA)<sub>2</sub>(MSC)<sub>2</sub>] (22)</b>	—	—	211
<b>[Ni(MSC)<sub>3</sub>](PA)<sub>2</sub> (20)</b>	—	—	217
<b>[Cu(H<sub>2</sub>O)<sub>2</sub>(MSC)<sub>2</sub>](HTNR)<sub>2</sub> (24)</b>	119	—	179
<b>[Zn(H<sub>2</sub>O)<sub>2</sub>(MSC)<sub>2</sub>](HTNR)<sub>2</sub> (25)</b>	134	—	195
<b>[Mn(HTNR)<sub>2</sub>(MSC)<sub>2</sub>] (26)</b>	—	—	184
<b>[Co(H<sub>2</sub>O)<sub>2</sub>(MSC)<sub>2</sub>](HTNR)<sub>2</sub> (27)</b>	155	—	205
<b>[Ni(H<sub>2</sub>O)<sub>2</sub>(MSC)<sub>2</sub>](HTNR)<sub>2</sub> (28)</b>	172	—	193

Onset temperatures at a heating rate of 5 °C min<sup>-1</sup> [a] endothermic peak, which indicates melting, vaporization, dehydration or loss of coordinating MSC molecules; [b] exothermic peak, which indicates decomposition.

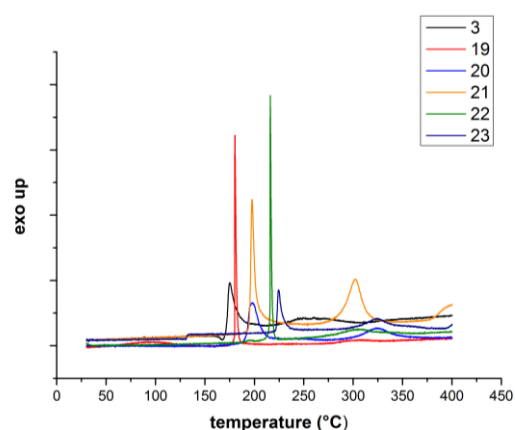


**Figure 11** DTA plot (5 °C min<sup>-1</sup>) comparison of the picrate compounds **3** and **19–23**.

Most of the styphnate complexes showed similar thermal stabilities in comparison with the picrates (Figure 13) but crystallized in different complex structures. Instead of coordinating trinitrobenzene derivative ligands, complexes with two aqua molecules were obtained. Dehydration indicated by an

## FULL PAPER

endothermic peak in the DTA plots (Figure 12) can be achieved by heating shown through weight loss during the TGA measurements (Figure 10).

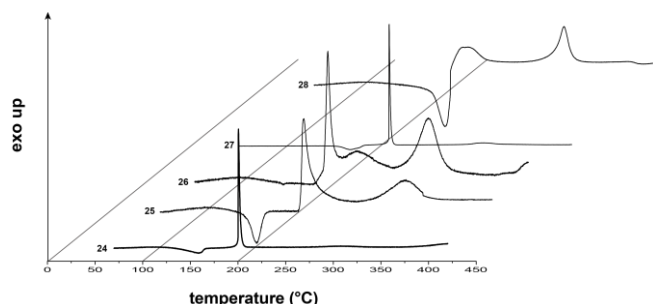


**Figure 12** DTA plots ( $5^\circ \text{ min}^{-1}$ ) of the styphnate complexes **24–28**.

The sensitivities toward impact, friction and electrostatic discharge for the compounds were determined according to BAM standards. In addition, the compounds have been classified in accordance to the “UN Recommendations on the Transport of Dangerous Goods” using the measured values. An overview of the sensitivities is given in Table 3. The uncoordinated free ligand **1** can be considered as “insensitive” with values greater than 40 J for impact, greater than 360 N for friction and an ESD value of 1.50 J. For complete energetic categorization of compound **1**, we calculated the enthalpy of formation to be  $-205 \text{ kJ mol}^{-1}$ .<sup>[31]</sup> So the compound is formed exothermically in contrast to the condensed phase heat of formation of monomethylhydrazine ( $54.1 \text{ kJ mol}^{-1}$ ).<sup>[32]</sup>

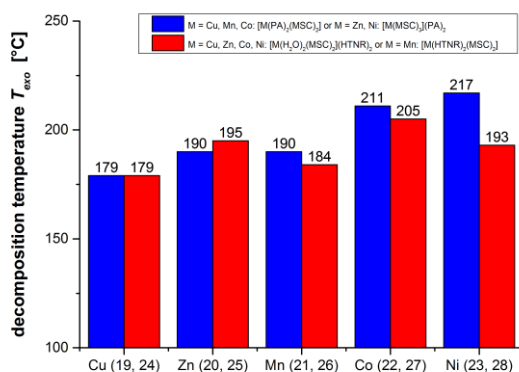


**Figure 13** Comparison of the exothermic decomposition temperatures of picrate complexes with styphnate coordination compounds.

**Table 3.** Sensitivities toward impact, friction and ESD of **1**, **3–12**, **14–15** and **17–28**.

	IS (J) <sup>[a]</sup>	FS (N) <sup>[b]</sup>	ESD (J) <sup>[c]</sup>	grain size (μm)
<b>1</b>	> 40	> 360	1.50	< 100
<b>3</b>	> 40	160	0.65	< 100
<b>4</b>	> 40	> 360	1.50	< 100
<b>5</b>	> 40	> 360	1.50	< 100
<b>6</b>	> 40	324	1.50	< 100
<b>7</b>	2	24	0.07	< 100
<b>8</b>	10	> 360	1.50	< 100
<b>9</b>	> 40	> 360	1.50	< 100
<b>10</b>	> 40	> 360	1.50	< 100
<b>11</b>	> 40	160	0.30	< 100
<b>12</b>	25	> 360	0.60	< 100
<b>14</b>	40	> 360	1.25	< 100
<b>15</b>	10	216	1.00	< 100
<b>17</b>	> 40	> 360	1.50	< 100
<b>18</b>	10	< 60	0.10	< 100
<b>19</b>	30	> 360	0.30	< 100
<b>20</b>	10	360	1.00	< 100
<b>21</b>	9	288	0.55	< 100
<b>22</b>	5	288	0.30	< 100
<b>23</b>	10	> 360	0.75	< 100
<b>24</b>	> 40	> 360	0.40	< 100
<b>25</b>	> 40	> 360	1.00	< 100
<b>26</b>	25	324	0.60	< 100
<b>27</b>	> 40	> 360	1.50	< 100
<b>28</b>	> 40	> 360	1.50	< 100

[a] Impact sensitivity according to the BAM drophammer (method 1 of 6); [b] friction sensitivity according to the BAM friction tester (method 1 of 6); [c] electrostatic discharge sensitivity (OZM ESD tester); Impact: insensitive > 40 J, less sensitive  $\geq 35$  J, sensitive  $\geq 4$  J, very sensitive  $\leq 3$  J; Friction: insensitive > 360 N, less sensitive = 360 N, sensitive < 360 N and > 80 N, very sensitive  $\leq 80$  N, extremely sensitive  $\leq 10$  N. According to the UN Recommendations on the Transport of Dangerous Goods.

The sulfate, chloride and nitrate complexes are insensitive against impact, friction and ESD (except compound **6**, which is sensitive toward friction). In most cases, substitution of these anions with perchlorates, azides, picrates or styphnates causes higher sensitivities toward impact, friction and ESD (impact: 2–40 J, friction: 24–360 N; ESD: 0.07–1.50 J). All water-free compounds with coordinating picrates or styphnates are more sensitive toward mechanical stimuli than their aqua ligand-containing analogs. Compound **7**, which behaves like a primary explosive, can be classified as very sensitive toward impact and friction, but it is still safe to handle, which makes it a very suitable initiating substance. The sensitivity toward impact of the  $[\text{M}^{\text{II}}(\text{PA})_2(\text{MSC})_2]/[\text{M}^{\text{II}}(\text{MSC})_3(\text{PA})_2]$  complexes (Figure 14) increases in the order:  $\text{Cu}^{2+} < \text{Zn}^{2+} < \text{Ni}^{2+} < \text{Mn}^{2+} < \text{Co}^{2+}$  and in the following order toward friction:  $\text{Cu}^{2+} \approx \text{Ni}^{2+} < \text{Zn}^{2+} < \text{Mn}^{2+} < \text{Ni}^{2+}$ . Incorporation of aqua ligands in the styphnate complexes **24/25** and **27/28** leads to an increase in stability toward mechanical stimuli but decreases its energetic character compared to the relating water-free picrate complexes (Figure 14).

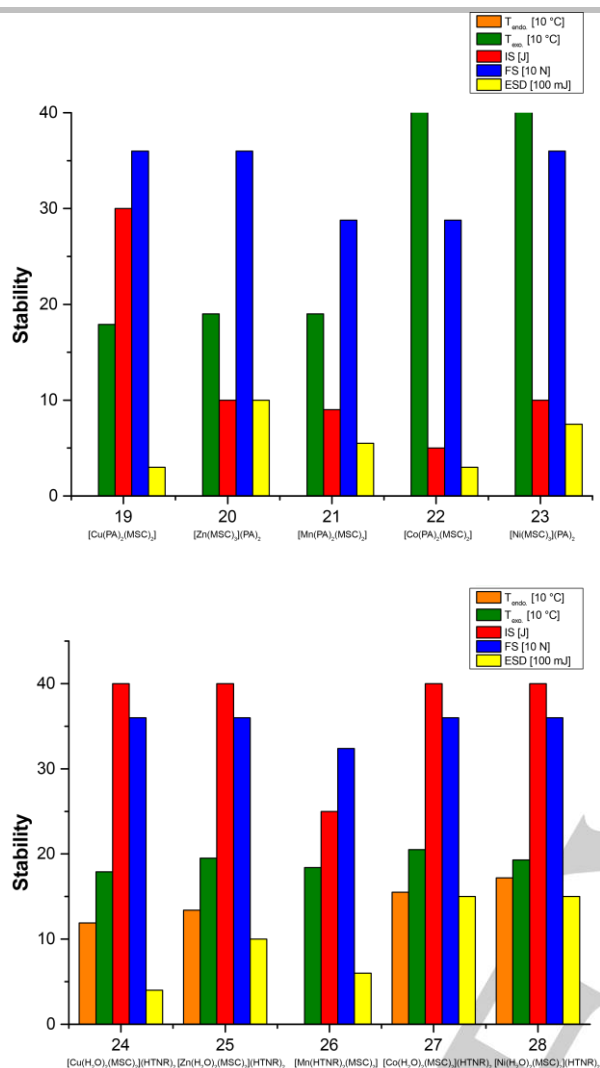


**Figure 14** Stabilities of the picrate and styphnate coordination compounds 19–28.

Hot needle and hot plate tests of the most promising compound **7** showed a sharp deflagration in both tests (Figure 15). The sample was fixed on a copper plate underneath adhesive tape and initiated by a red hot needle. Strong deflagration or detonation of the compound usually indicates a valuable primary explosive. The safe and straightforward hot plate test shows only the behaviour of the unconfined sample toward fast heating on a copper plate. It does not necessarily allow any conclusions on a compound's capability as a suitable primary explosive.



**Figure 15** Moment of deflagration of compound **7** during the hot needle test (left) and hot plate test (right).

Based on the positive results of the hot needle and hot plate tests, the initiation capability of compound **7** toward pentaerythritol tetranitrate (PETN) as secondary explosive was investigated. A copper shell with a diameter of 7 mm and length of 88 mm was filled with 200 mg sieved PETN (grain size 100–500  $\mu\text{m}$ ) and pressed with a weight of 8 kg. 50 mg of the primary explosive was subsequently loosely filled on top of the main charge. To examine the influence of pressing of the primary explosive on the initiation capability, two experiments were conducted a.) with pressing and b.) without. The shell was sealed by an insulator, placed in a retaining ring, which was soldered to a copper witness plate with a thickness of 1 mm and finally initiated by a type A electrical igniter (Figure 16).



**Figure 16** Schematic test setup (left); copper shell and plate before the initiation capability test (right).

A positive test is indicated by a hole in the copper plate and fragmentation of the shell caused by a deflagration-to-detonation transition (DDT) of the secondary explosive. In the case of compound **7**, two different results are observed depending on the pressing of the sample and the related loading density (Figure 17). A negative test, represented by a nearly undamaged copper plate, was obtained after loosely filling the primary into the shell. Pressing of the sample on top of the main charge led to a positive result and complete detonation of PETN proofed by a hole in the plate.

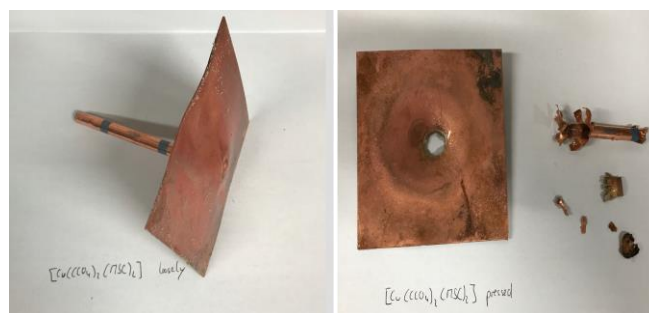


**Figure 17** Negative (left) and positive (right) results of the PETN initiation tests.

### Toxicity

The toxicity of compound **1** was determined using the known luminescence marine bacterium *Vibrio fischeri* in order to estimate the potential toxicological impact of the corresponding complexes.<sup>[33]</sup> With a value of 1.48  $\text{g L}^{-1}$  for the half maximal

## FULL PAPER

effective concentration  $EC_{50}$  after 30 min, the compound can be considered as non-toxic (toxicity level after 30 min incubation: very toxic  $< 0.10 \text{ g L}^{-1}$ ; toxic  $0.10\text{--}1.00 \text{ g L}^{-1}$ ; non-toxic  $> 1.00 \text{ g L}^{-1}$ ).<sup>[34]</sup>

## Laser initiation

In recent years, more and more research groups all over the world have been working intensively on new laser ignitable energetic materials.<sup>[35-37]</sup> The laser initiation shows many advantages compared to conventional methods like mechanical stimuli or heat and investigated compounds do not require high sensitivities toward the customary stimuli. Consequently, laser ignitable explosives with high performance, high thermal stability and no impact on the environment can be used as insensitive but powerful energetic materials to allow much safer handling and prevent undesired initiations. About 15 mg of the carefully pestled complex to be investigated were filled into a transparent plastic cap, pressed with a pressure force of 1 kN and sealed by a UV-curing adhesive. The laser initiation experiments were carried out with a 45 W InGaAs laser diode operating in the single-pulsed mode. The diode was connected to an optical fiber with a core diameter of 400  $\mu\text{m}$  and a cladding diameter of 480  $\mu\text{m}$ . The optical fiber was coupled via a SMA type connector directly to the laser and to a collimator. This collimator was linked to an optical lens, which was positioned in its focal distance ( $f = 29.9 \text{ mm}$ ) to the sample. The lens was protected from the explosive by a sapphire glass. The confined samples were irradiated at a wavelength of 915 nm, a voltage of 4 V and varying parameters regarding pulse length (0.1 ms or 15 ms) and current (8 A or 9 A). The combined current and pulse length result in an approximately energy output of 0.20 mJ (0.1 ms/8A) and 34 mJ (15 ms/9A). Only selected compounds with promising properties (**7**, **8** and **18**) were tested toward laser irradiation and showed different responses depending on the used metal(II) and anion. A summary of the test results is given in Table 4. All investigated complexes could be initiated showing detonations for **7** and **18** (Figure 18) and decomposition for compound **8** under the applied laser parameters.

**Table 4** Results of the laser ignition tests.

	0.1 ms/8 A	15 ms/9 A
<b>7</b>	det.	–
<b>8</b>	dec.	–
<b>18</b>	x	det.

(–: not tested, x: no ignition, dec.: decomposition, deflag.: deflagration, det.: detonation). Operating parameters: current  $I = 8\text{--}9 \text{ A}$ ; voltage  $U = 4 \text{ V}$ ; theoretical maximal output power  $P_{\text{max}} = 45 \text{ W}$ ; theoretical energy  $E_{\text{max}} = 0.20\text{--}34 \text{ mJ}$ ; wavelength  $\lambda = 915 \text{ nm}$ ; pulse length  $\tau = 0.1\text{--}15 \text{ ms}$ .

Different laser initiation thresholds could be observed for the complexes expressed by varying outcomes and required energy inputs. Copper(II) complex **7** detonated at the lowest possible initiation energy configurable in the settings of the laser device. The compound exhibits slightly increased sensitivities against mechanical stimuli but is still safe to handle and therefore a promising candidate for future laser ignition systems.



**Figure 18** Moment of detonation of compound **7**.

## UV-Vis spectroscopy

In order to get a deeper insight into the laser initiation mechanism of energetic materials solid state UV-Vis spectra for the coordination compounds **7**, **8** and **18** were recorded in the wavelength region 350–1000 nm (Figure 19). In addition, the influence of different anions on the absorption for copper(II) complexes was investigated and compared to each other (Figure S13). An overview of the observed optical properties is given in Table 5.

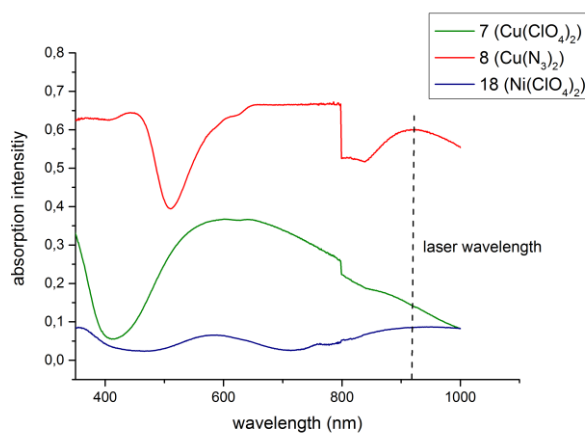


**Figure 19** UV-Vis spectra in the solid state of complexes **7**, **8** and **18**. The step in the absorption intensity at 800 nm in the spectra is caused by a detector change. The UV-Vis spectra have only qualitative character.

All analyzed complexes showed characteristic absorptions in the near-infrared, visible and UV region correlating with their observed complementary colors. Depending on the transition metal ( $\text{Cu}^{2+}$  vs.  $\text{Ni}^{2+}$ ) or coordination environment (blue  $\text{Cu}(\text{ClO}_4)_2$  (**7**) vs. green  $\text{Cu}(\text{N}_3)_2$  (**8**)) different d-d transitions can be found. As expected, the blue copper(II) complexes **4–7** differ only minimally from each other, which can be explained by their similar coordination environment.

**Table 5** Optical properties of **14-27**, **31** and **36**.

## FULL PAPER

	M	color	$\lambda_{d-d}^{[a]}$	$\lambda_{915}/\lambda_{d-d}^{[b]}$
4	Cu <sup>II</sup>	blue	646	0.51
5	Cu <sup>II</sup>	blue	642	0.51
6	Cu <sup>II</sup>	blue	603	0.46
7	Cu <sup>II</sup>	blue	602	0.40
8	Cu <sup>II</sup>	green	786	0.89
18	Ni <sup>II</sup>	blue	581, 952	0.98

[a] absorption intensity maximum wavelength, which can be assigned to electron d-d excitations in the measured range of 350–1000 nm; [b] quotient of the absorption intensity at the laser wavelength and the intensity at the d-d absorption wavelength.

The nature of the laser ignition process (e.g. thermally, electronically or combined) and the related requirements of compounds to be laser ignitable are still not fully understood.<sup>[38]</sup> Looking at the absorption intensity of the coordination compounds at the irradiated wavelength of 915 nm (Figure 19), one could possibly derive a direct connection to the performed laser ignition since all complexes could be initiated. However, the laser initiation capability depends not only on the absorption but also on multiple other factors like crystal structure or the coordination environment.<sup>[29]</sup> It can be concluded that deflagration or detonation of the complexes after exposure to laser irradiation occurs possibly if the compounds possess high mechanical sensitivities. Because of the influence of the metal, anion and ligand on the laser initiation process, as well as the mechanism itself has not been clarified yet, future investigations will be needed to fully understand the laser initiation of energetic materials.

## Conclusions

Methylsemicarbazide (**1**, MSC), a methyl derivative of semicarbazide and member of the prominent carbazide family, was prepared in a facile one-step reaction by treatment of trimethylsilylisocyanate with methylhydrazine in a high yield of 95%. Toxicity determination showed no toxicity of **1** toward aquatic life, which makes it a suitable candidate as ligand in environmental benign complexes for various applications. In comparison to hydrazine and methylhydrazine as ligands (both show high toxicities), significantly less sensitive compounds are obtained which might be a reason of the negative heat of formation ( $-205 \text{ kJ mol}^{-1}$ ) of **1**. In the present extensive study 25 new coordination compounds, with **1** as the ligand, were synthesized and investigated. Coordination causes intramolecular rotation of the bidentate ligand and leads to an increase in density in comparison to the free compound **1**. Obtained complexes are composed of a 3d transition metal (Mn, Co, Ni, Cu, Zn), methylsemicarbazide and varying anions ( $\text{SO}_4^{2-}$ ,  $\text{Cl}^-$ ,  $\text{NO}_3^-$ ,  $\text{ClO}_4^-$ ,  $\text{N}_3^-$ , picrates, styphnates). Attempts using Fe(II) and Fe(III) salts failed. The concept of energetic coordination compounds (ECCs), which are obtained by including nitrate, perchlorate, nitrophenolates and azide anions, is a brilliant, inexpensive and simple strategy in order to find new laser-ignitable and eco-friendly primary explosives. Energetic and optical properties can be easily adjusted by variation of the building blocks (metal, ligand, anion). Most of the complexes showed exothermic decomposition temperatures higher or close to 180 °C during differential thermal analysis (DTA)

measurements. Thermal gravimetric analysis (TGA) of selected compounds gave new insights into possible decomposition pathways at elevated temperatures. Highest stabilities toward temperature were observed for nickel(II) and cobalt(II) complexes, while highest stabilities toward physical stress for manganese(II) and zinc(II) complexes. Additionally, low temperature X-ray structure elucidation for 22 compounds was achieved and allowed the correlation between crystal structure and mechanical stabilities (e.g. the bridging azido ligand in the low-performing copper(II) complex **8** vs. the highly sensitive perchlorate complex **7**). All investigated picrate complexes crystallized water-free and showed higher sensitivities in comparison to their diaqua containing styphnate analogs. Compound **7** has a high thermal stability (186 °C) and shows manageable sensitivities for a primary explosive. Further investigation in a PETN filled copper shell proved its suitability as lead-free alternative. The successful ignition (observing detonation) of PETN makes copper(II) complex **7** to an interesting candidate for future primary explosive applications. It can be prepared by a simple, low-cost and upscalable reaction. Also, non-classical initiation tests by laser irradiation at a wavelength of 915 nm showed detonation of complex **7** after irradiation at the lowest applicable energy input of the laser setup (0.2 mJ).

## Acknowledgements

We acknowledge the financial support of this work, which was provided by the Ludwig-Maximilian University of Munich (LMU). The authors also want to thank Mr. Stefan Huber for sensitivity measurements, Mrs. Cornelia Unger for toxicity assessments, Mr. Josh Bauer for proofreading and Mrs. Chantal von der Heide for contribution. In addition, the authors are indebted to Prof. Thomas M. Klapötke and gratefully acknowledge his financial and technical support.

**Keywords:** methylsemicarbazide • coordination chemistry • transition metal complexes • primary explosives • laser ignition

- [1] T. W. Myers, K. E. Brown, D. E. Chavez, R. J. Scharff, J. M. Veauthier, *Inorg. Chem.* **2017**, *56*, 2297–2303.
- [2] S. Seth, K. A. McDonald, A. J. Matzger, *Inorg. Chem.* **2017**, *56*, 10151–10154.
- [3] M. Freis, T. M. Klapötke, J. Stierstorfer, N. Szimhardt, *Inorg. Chem.* **2017**, *56*, 7936–7947.
- [4] S. Li, Y. Wang, C. Qi, X. Zhao, J. Zhang, S. Zhang, S. Pang, *Angew. Chem., Int. Ed.* **2013**, *52*, 14031–14035.
- [5] K. D. Oyler, in *Green Energetic Materials*, John Wiley & Sons, Ltd, **2014**, pp. 103–132.
- [6] Y. Tang, C. He, L. A. Mitchell, D. A. Parrish, J. M. Shreeve, *Angew. Chem., Int. Ed.* **2016**, *55*, 5565–5567.
- [7] D. G. Piercey, D. E. Chavez, B. L. Scott, G. H. Imler, D. A. Parrish, *Angew. Chem., Int. Ed.* **2016**, *55*, 15315–15318.
- [8] R. Haiges, K. O. Christe, *Inorg. Chem.* **2013**, *52*, 7249–7260.
- [9] R. Matyás, J. Pachman, in *Primary Explosives*, Springer, Heidelberg **2013**.
- [10] M. A. Ilyushin, I. V. Tselinsky, I. V. Shugalei, *Cent. Eur. J. Energ. Mater.* **2012**, *9*, 293–327.
- [11] M. Joas, T. M. Klapötke, J. Stierstorfer, N. Szimhardt, *Chem. - Eur. J.* **2013**, *19*, 9995–10003.
- [12] J. Zhang, Y. Du, K. Dong, H. Su, S. Zhang, S. Li, S. Pang, *Chem. Mat.* **2016**, *28*, 1472–1480.

## FULL PAPER

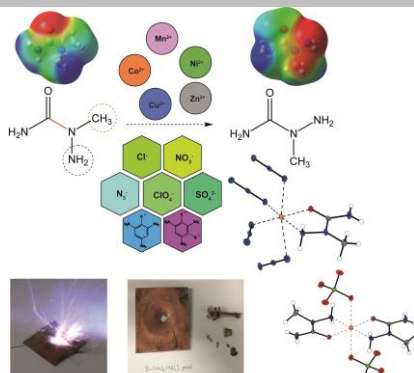
- [13] B. Hariharanath, K. S. Chandrabhanu, A. G. Rajendran, M. Ravindran, C. B. Kartha, *Def. Sci. J.* **2006**, *56/3*, 383–389.
- [14] T. Curtius, K. Heidenreich, *Chem. Ber.* **1894**, *27*, 55.
- [15] M. B. Labib, P. F. Lamie, *Med. Chem. Res.* **2016**, *25*, 2607–2618.
- [16] R. J. W. Cremyln, J. L. Turner, *J. Chem. Soc., C* **1970**, 2629–2631.
- [17] W.-C. Tong, J.-C. Liu, Q.-Y. Wang, L. Yang, T.-L. Zhang, *Z. Anorg. Allg. Chem.* **2014**, *640*, 2991–2997.
- [18] a.) V. P. Sinditskii, A. E. Fogelz'ang, M. D. Dutov, V. V. Serushkin, S. P. Yarkov, B. S. Svetlov, *Zh. Neorg. Khim.* **1986**, *31*, 1759–1765; b.) V. P. Sinditskii, A. E. Fogelz'ang, M. D. Dutov, V. I. Sokol, V. V. Serushkin, B. S. Svetlov, M. A. Porai-Koshits, *Zh. Neorg. Khim.* **1987**, *32*, 1944–1949; c.) M. B. Talawar, A. P. Agrawal, J. S. Chhabra, S. N. Asthana, *J. Hazard. Mater.* **2004**, *113*, 57–65.
- [19] M. Joas, T. M. Klapötke, *Propellants, Explos., Pyrotech.* **2015**, *40*, 246–252.
- [20] C. Sitong, G. Weiming, Z. Bo, Z. Tonglai, Y. Li, *Polyhedron* **2016**, *117*, 110–116.
- [21] X. Fu, F. He, Y. Li, L. Liu, Y. Mi, Y.-C. Xu, G. Xun, Z. Yu, J. Y. Zhang, M. Dai, Novartis AG, Switz. **2011**, p. 143pp.
- [22] A. Shibayama, R. Kajiki, M. Kobayashi, T. Mitsunari, A. Nagamatsu, Kumiai Chemical Industry Co., Ltd., Japan; Ihara Chemical Industry Co., Ltd. **2012**, p. 226pp.
- [23] Crystallographic data for the structures have been deposited with the Cambridge Crystallographic Data Centre. Copies of the data can be obtained free of charge on application to The Director, CCDC, 12 Union Road, Cambridge CB2 1EZ, UK (Fax: int.code\_(1223)336-033; e-mail for inquiry: fileserv@ccdc.cam.ac.uk; e-mail for deposition: [deposit@ccdc.cam.ac.uk](mailto:deposit@ccdc.cam.ac.uk)).
- [24] P. Domiano, M. A. Pellinghelli, A. Tiripicchio, *Acta Crystallogr., Sect. B* **1972**, *28*, 2495–2498.
- [25] J. E. Worsham, Jr., H. A. Levy, S. W. Peterson, *Acta Crystallogr.* **1957**, *10*, 310–323.
- [26] A. Cabort, B. Therrien, K. Bernauer, G. Süß-Fink, *Inorg. Chim. Acta* **2003**, *349*, 78–84.
- [27] K. C. Patil, *J. Chem. Sci.*, **1986**, *96*, 459–464.
- [28] R. A. F. Sherriff and A. K. Galwey, *J. Chem. Soc. A*, **1967**, 1705–1708.
- [29] J. Stierstorfer, N. Szimhardt, M. H. H. Wurzenberger, L. Daumann, A. Beringer, *J. Mater. Chem. A*, **2017**, *5*, 23753–23765.
- [30] M. Joas, PhD thesis; Ludwig-Maximilians Universität München, **2014**.
- [31] a) CBS-4M was applied for the electronic enthalpy; atomization method for conversion to gas phase enthalpy of formation and Trouton's rule for computing the sublimation enthalpy; b) T. Altenburg, T. M. Klapötke, A. Penger, J. Stierstorfer, *Z. Anorg. Allg. Chem.* **2010**, *636*, 463–471.
- [32] NIST <http://webbook.nist.gov/cgi/cbook.cgi?ID=C302012&Mask=1E9F>, Accessed October 2017.
- [33] G. I. Sunahara, S. Dodard, M. Sarrazin, L. Paquet, G. Ampleman, S. Thiboutot, J. Hawari, A. Y. Renoux, *Ecotoxicol. Environ. Saf.*, **1998**, *39*, 185–194.
- [34] C. J. Cao, M. S. Johnson, M. M. Hurley, T. M. Klapötke, *JANNAF J. Propuls. Energet.*, **2012**, *5*, 41–51.
- [35] T. W. Myers, J. A. Bjorgaard, K. E. Brown, D. E. Chavez, S. K. Hanson, R. J. Scharff, S. Tretiak, J. M. Veauthier, *J. Am. Chem. Soc.* **2016**, *138*, 4685–4692.
- [36] M. A. Ilyushin, I. V. Tselinksi, *Zh. Prikl. Khim.* (S.-Petersburg, Russ. Fed.) **2000**, *73*, 1233–1240.
- [37] M. Freis, T. M. Klapötke, J. Stierstorfer, N. Szimhardt, *Inorg. Chem.* **2017**, *56*, 7936–7947.
- [38] E. D. Aluker, A. G. Krechetov, A. Y. Mitrofanov, D. R. Nurmukhametov, M. M. Kuklja, *J. Phys. Chem. C*, **2011**, *115*, 6893–6901.

## FULL PAPER

## Entry for the Table of Contents

## FULL PAPER

Methylsemicarbazide (MSC) was successfully demonstrated as suitable building block in the formation of 25 new energetic coordination compounds (ECC). The further clever selection of late 3d metals, co-solvents and anions yielded a wide choice of different functional materials partly suitable for laser ignition or as classical primary explosive.



Norbert Szimhardt, Jörg Stierstorfer\*

Page No. – Page No.

Methylsemicarbazide as Ligand in  
Late 3d Transition Metal Complexes